SUPPLEMENTAL MATERIAL

Single biallelic locus. Letting allele **A** (denoted as state 1 below) have a fractional selective advantage s over allele **a** (denoted as state 0), and the mutation rates from the former to the latter and vice versa be u_{10} and u_{01}, respectively, the full stationary distribution of allele frequencies for this two-allele system has already been derived (1, 2). Letting x be the frequency of the deleterious allele **a**, $U_{01} = 2N_e u_{01}$, $U_{10} = 2N_e u_{10}$, and $S = 2N_e s$, the continuous distribution is given by

$$\phi(x) = C x^{U_{10}-1}(1-x)^{U_{01}-1} e^{-Sx} \tag{S1a}$$

with normalization constant

$$C = \frac{\Gamma(U_{01}+U_{10})}{\Gamma(U_{01}) \cdot \Gamma(U_{10}) \cdot {}_1F_1(U_{10}; (U_{01}+U_{10}); -S)}, \tag{S1b}$$

where Γ denotes the gamma function, and ${}_1F_1$ is the confluent hypergeometric function, defined respectively as Equations 6.1.2 and 13.1.2 in Abramowitz and Stegun (3). Equation (S1a) can be viewed as the long-term probability of a single lineage residing at frequency x or equivalently as the fraction of independent populations residing at frequency x at any particular time. Integrating Equation (S1a) over the full range of x yields the long-term mean frequency of the deleterious allele

$$\overline{p}_0 = \frac{\mu_{10} \cdot {}_1F_1[(U_{10}+1); (U_{01}+U_{10}+1); -S]}{(\mu_{01}+\mu_{10}) \cdot {}_1F_1[U_{10}; (U_{01}+U_{10}); -S]}, \tag{S2}$$

with that of the beneficial allele being $\overline{p}_1 = 1 - \overline{p}_0$ (1, 4). With a haploid, single-locus model, $\overline{p}_1$ is equivalent to the long-term probability that a single randomly sampled individual has the highest-fitness genotype.

Although Equation (S1a) yields an essentially perfect fit with data from simulations of a standard Wright-Fisher model with reversible mutation, drift, and selection (Figure 2, Main Text), it is cumbersome mathematically and visual inspection does not lead to a transparent interpretation. (The C++ code for this and all other simulations is available from the author upon request). Thus, it is common in population genetics to use one of two alternative approximations. One extreme view is that drift is weak enough relative to mutation and selection that the population can be treated as effectively infinite in size. Under this deterministic model, a stable equilibrium allele frequency generally arises, and there is no divergence among populations provided the underlying evolutionary forces remain constant. The single point equilibrium

frequency for the deleterious allele **a** is

$$\widetilde{p}_0 = \frac{[u_{01} + u_{10} + s(1 - u_{01})] - \sqrt{[u_{01} + u_{10} + s(1 - u_{01})]^2 - 4su_{10}}}{2s}. \tag{S3a}$$

Because both the selection coefficient and the mutation rates are < 1, the latter generally by orders of magnitude, the previous expression reduces to

$$\widetilde{p}_0 \simeq \frac{u_{10}}{u_{01} + u_{10} + s}. \tag{S3b}$$

A second approach relies on models that assume finite populations experiencing low enough rates of mutation and high enough strength of selection that polymorphisms are almost never present, with fixation of alternative monomorphic states being the norm. Under this view, over a long enough time period, there is a steady-state flux between alternative fixed states. Letting p_0^* and p_1^* be the equilibrium frequencies such that the net rates of flux are equal in both directions, the final solution satisfies

$$p_0^* \cdot (Nu_{01}) \cdot f_{01} = p_1^* \cdot (Nu_{10}) \cdot f_{10}, \tag{S4}$$

where the terms in parentheses denote the rates of origin of mutations from their respective source populations, and f_{01} and f_{10} denote the probabilities of fixation of newly arisen beneficial and deleterious alleles. From standard diffusion theory (5, 6),

$$f_{01} = \frac{1 - e^{-2(N_e/N)s}}{1 - e^{-2N_e s}}, \tag{S5}$$

with f_{10} defined in the same way with the sign of s changed. Using the identity $f_{01}/f_{10} = e^S$, which holds in the limit of large N (the more general result being $e^{S[1-(1/N)]}$), where $S = 2N_e s$, and letting $\beta = u_{01}/u_{10}$ be the ratio of mutation rates, the expected frequency of the beneficial allele is

$$p_1^* \simeq \frac{\beta e^S}{1 + \beta e^S}. \tag{S6}$$

Computer simulations. For all conditions modeled, computer simulations were performed using a "Wright-Fisher" framework. Custom software written in C++ to carry out the specialized goals of the work is available from the author upon request. The validity of the code was evaluated by comparing outputs under a range of conditions for which analytical results were available, e.g., the cases of neutrality and small-population size limits where the results of the

sequential model (described in the text) apply. As all analyses involved nonrecombining genomes and mutations with constant and additive fitness effects, individuals were simply characterized by their numbers of $-/+$ alleles. The basic simulation procedure involved a repetitive cycle of three per-generation steps to iteratively generate the frequency distribution of individuals with the full range of possible mutation numbers (0 to L, with L genomic sites):

1) Starting with the genotype frequencies from the end of the preceding generation, mutation was imposed by deterministically transforming the frequencies of each class into three categories – the retained nonmutants, and those in the two adjacent classes. Given the low mutation rates employed, double mutants were ignored.

2) Selection was then imposed on the post-mutational distribution by multiplying the latter frequencies by the class-specific fitnesses scaled by the post-mutation mean population fitness. These fitnesses were defined by the various fitness functions described in the text, and the use of relative fitnesses ensures that the frequency distribution sums to 1.0 after selection.

3) The post-selection frequencies were then treated as expected values in the random drift process, whereby new frequencies were stochastically generated by random multinomial sampling to produce a new pool of N haploid individuals. At this point, all nonzero classes have frequencies that are integer multipliers of $1/N$. These frequencies then constituted the next generation to be re-entered into step 1.

The primary goal of the simulations was to determine the long-term mean and variance of the number of $-$ alleles per individual in the population, given the mutation function, the selection function, and the absolute population size (N). To achieve this, a single, long string of generations was performed, with statistics generally being compiled every $0.1N$ generations; under neutrality, fixation of a new mutation occurs in $2N$ generations on average, so this interval reduces the computational time spent on nonindependent data. For each simulation, the starting distribution was based on the analytical predictions of the sequential model or on the expectations of the deterministic single-locus model, both described in the text. For each run, prior to compiling simulation statistics, a burn-in period of $1000N$ generations was imposed, i.e., long enough for 500 fixations per site under neutrality. Recordings of the frequency distribution and its mean and variance were then recorded for 10^8 to 10^9 time points, with the requirement that the cumulative mean and variance of the distribution for the number of mutations per individual stabilized to the point of $< 0.01\%$ change per recording. In no case did the final result

depend on the starting distribution or the interval between data recording, consistent with the overall runs being long enough to achieve equilibrium.

As illustrated in the main text, for any pair of mutation and selection functions, simulations were performed for population sizes ranging from 1.3×10^4 to 2.0×10^8 individuals. Owing to the length of the individual runs (up to several days), for some of the very largest population sizes, it was necessary to scale down the population size N in a way that kept Ns and Nu constant, i.e., by simultaneously reducing N by a factor of x and increasing u and s by the same factor. This keeps the power of selection and mutation relative to drift constant, and based on diffusion theory is expected to yield the same results in shorter time periods, as was verified in simulations prior to adapting this strategy. In addition, as the number of loci imposed ranged up to $L = 10^6$, whereas at equilibrium the population typically occupied only a small range of the possible classes, the upper and lower bounds of the distributions were tracked each generation so that all zero classes except those adjacent to the lowest and highest occupied classes could be ignored. Although these bounds stochastically vary across generations, such treatment dramatically speeds up the simulations by minimizing the time spent on nonexistent classes.

Large numbers of loci. Attempts were made to derive an analytical expression for the equilibrium genotype distribution under the joint influence of selection, mutation, and random genetic drift in the case of large numbers of loci (L), and although the outcome was not fully satisfactory, some relationships that emerged may be useful to future investigators. As a starting point, one might draw insight from the limiting case of an infinite population size, infinite sites, and an absence of beneficial mutations, where it is known that the population settles into a selection-mutation balance for the distribution of numbers of individuals with different numbers of deleterious alleles. In this case, the equilibrium distribution is Poisson in form, defined by the parameter U_d/s, where U_d (assumed to be independent of the number of pre-existing mutations under the infinite-sites model) is the genome-wide rate of deleterious mutation (7); the expected fraction of individuals in the best class (zero deleterious mutations) is then $e^{-U_d/s}$.

There are, however, several problems with extending the Haigh model (7) here. First, with finite numbers of sites, U_d is not independent of an individual's genetic background, as the rate of deleterious mutation of an individual, $u_{10}(L-m)$, depends on its genotypic state. As the number

of + sites increases, the genome-wide deleterious mutation rate increases, whereas the mutation rate to further beneficial alleles declines. Second, unless the population size is unrealistically high, the expected number of individuals in the best class will be orders of magnitude below 1, and the relationship between the mean frequency of + alleles/site and the position of the nose of the distribution is unclear. Third, the Haigh model does not allow for the recovery of lost classes by back-mutation. It has been argued that with a more complete model, the steady-state distribution likely resembles a shifted Poisson distribution (8), with parameter $U_d/(s+u_{01})$, but this again assumes an infinite-sites / infinite population-size model.

Because selection operates on genetic variation, a key component driving the scaling patterns in Figure 5 must be the expected standing level of within-population genetic variance for the trait, σ_m^2. In principle, the long-term average value of this variance can be approximated by use of a modified version of a recursion equation that treats m as a quantitative trait,

$$\sigma_m^2(t+1) \simeq (1-s)\cdot\left\{\lambda\sigma_m^2(t) + u_{10}\mu_m(t) - u_{01}[L-\mu_m(t)]\right\}, \tag{S7}$$

where $\lambda = 1-(1/N_e)$ is the fraction of genetic variation retained after a generation of drift, and the last two terms are the rates of change of variance in the number of + sites by mutation (9; their Equation 1b). Solution of this expression leads to the equilibrium expectation

$$\widetilde{\sigma}_m^2 = \frac{(1-s)[u_{10}\widetilde{\mu}_m - u_{01}(L-\widetilde{\mu}_m)]}{1-\lambda(1-s)}. \tag{S8a}$$

Jain and John (10) analyzed a model similar to that employed here, but assumed an infinite number of sites and infinite population size. Modifying their genome-wide mutation rates to allow for finite numbers of sites leads to

$$\widetilde{\sigma}_m^2 \simeq \frac{u_{10}\widetilde{\mu}_m - u_{01}(L-\widetilde{\mu}_m)}{s}, \tag{S8b}$$

which is consistent with Equation (S8a) for $N_e = \infty$ and small s. The same expression can be derived from another infinite-sites model (11; their p. 1313) after suitable modification to a finite-sites scenario.

There are two unfortunate concerns with Equations (S8a,b). First, they are functions of the equilibrium mean number of + alleles, $\widetilde{\mu}_m$, which is the unknown that we are trying to determine. Second, for $N_e s \ll 1$ (the realm of effective neutrality), one would expect the variance to become saturated at large N_e, as all sites harbor a heterozygosity equivalent to that expected for an

infinite-sized population. However, as $N_e s \to 0$, $\widetilde{\sigma}_m^2 \to 2N_e L u_{01}/(1+\beta)$, growing without bounds with increasing N_e in Equation (S8a), whereas the actual neutral variance is

$$\widetilde{\sigma}_m^2 = \frac{2N_e u_{01} L}{1+\beta+N_e u_{10}(1+6\beta+\beta^2)}. \tag{S9}$$

where $\beta = u_{01}/u_{10}$. Equation (S9), which was confirmed by computer simulations with $s = 0$, has a limit of $2L\beta/(1+6\beta+\beta^2)$ at large N_e (which reduces to $L/4$ for $\beta = 1.0$).

Despite these caveats, when the observed equilibrium genotypic means from simulations are substituted, Equations (S8a,b) predict within-population variances that are in essentially perfect accord with simulated data, across the full range of evaluated N, s, and L (Figure S1a). Moreover, the simpler version, Equation (S8b) yields results almost identical to (S8a), demonstrating that most of the information on drift and selection resides in $\widetilde{\mu}_m$. These observations show that the overall approach is internally consistent, but do not solve the problem of obtaining $\widetilde{\mu}_m$ from first principles.

A parallel approach is to consider the dynamics of the mean $\widetilde{\mu}_m$ conditional on $\widetilde{\sigma}_m^2$. Again using a quantitative-genetic approach and an infinite-sites model, Lynch et al. (9; their Equation 1a) suggested that, in the absence of back-mutations, the rate of decline of the expected mean phenotype is $U_d(1-s) - s\lambda\widetilde{\sigma}_m^2$, which converts to $u_{10}\widetilde{\mu}_m(1-s) - s\lambda\widetilde{\sigma}_m^2$ under a finite-sites model at equilibrium. Noting that the recovery rate is $\simeq u_{01}(L - \widetilde{\mu}_m)$ and equating these two rates leads to the solution

$$\widetilde{\mu}_m = \frac{u_{01}L + s\lambda\widetilde{\sigma}_m^2}{u_{01} + u_{10}(1-s)}. \tag{S10}$$

When the average variances from simulations, $\widetilde{\sigma}_m^2$, are substituted into this formula, the simulated long-term means are predicted to a high degree of accuracy, again showing the internal consistency of this approach (Figure S1b).

Because Equation (S8b) yields accurate predictions of the variance given an estimate of the mean, and Equation (S10) gives an accurate estimate of the mean given an estimate of the variance, one would expect that their joint solution would yield an accurate estimate of $\widetilde{\mu}_m$ based on the mutation rates, s, and N, but this proves not to be the case. It is unclear why the combination of two very well-performing expressions yields an unsatisfactory result, but ignored higher-order moments may be involved. Previous work on a model very similar to the one presented here (11-13), with reversible mutation in a finite-sites / finite-population size framework and an exponential fitness function, yields various approximations that do not seem

to yield results relevant to the problem herein. For example, Woodcock and Higgs (12) provide an analytical approximation for the equilibrium frequency of + alleles, but the final result relies on the assumption of a binomial distribution of genotypic classes and yields an expression that is independent of L, neither of which is consistent with simulation results. Moreover, a modification of their derivations to allow for a Poisson distribution was unhelpful, probably because the distribution is more complex (11). Expressions for the location of the most-fit genotype have been arrived at by using a matching criterion for the rates of loss and gain of the nose of the distribution (11, 13), but these too have been found to map poorly to the mean phenotype for the parameter space used herein, as at large N a near optimal phenotype is nearly always present at low frequency even though the mean is much lower.

Gaussian directional selection. The exponential fitness function used in the bulk of the main text is one of many possible forms of directional selection. A commonly used alternative is the half-Gaussian function, which can be implemented by letting fitness be maximized when all alleles are +, with the strength of selection governed by ω, so that W_m is defined as in Equation (2) with the optimum $\theta = 0$. From Lynch (14), with large numbers of sites, the equilibrium mean number of deleterious alleles ($d = L - m$) per individual is

$$\widetilde{\mu}_d \simeq \frac{L(1-\eta)}{1 + (\widetilde{\sigma}_m^2/\sigma_S^2)}, \tag{S11}$$

where $\widetilde{\sigma}_m^2$ is defined in Equation (S9), and $\sigma_S^2 = (\omega^2 + \sigma_z^2)/(2N_e)$, where σ_z^2 is the average within-population phenotypic variance of the trait. For the combination of mutation rates and population sizes used here, $Nu \ll 1$, and from Equation (S9) the neutral level of variation can be approximated by $\widetilde{\sigma}_m^2 = 2NLu_{01}/(1+\beta)$. Letting $\sigma_z^2 = \widetilde{\sigma}_m^2$ then leads to an expression for the average equilibrium frequency of deleterious alleles,

$$\widetilde{p}_- = \frac{1}{1 + \beta + \dfrac{\beta}{[\omega^2(1+\beta)/(2N_eL)] + u_{01}}}. \tag{S12}$$

As with the exponential fitness function (in the main text), the structure of this expression suggests that the key determinants of the equilibrium mean frequency are the scaled selection intensity N_e/ω^2, the mutation bias β, and the number of sites in the linkage block L.

If an analytical solution of the response of the mean phenotype to the change in absolute population size N is to be obtained, the central remaining issue is again how N_e scales with these

factors. The scaling behavior cannot be the same as that for the exponential fitness function, as the gradient of selection under the Gaussian function shifts with the distance of the mean phenotype from the optimum. As can be seen in Figure S4, this results in less sharp inflections in the S-shaped response curves of the mean phenotype ($\mu_b = L - \mu_d$) to population-size increase.

As with the exponential fitness function, insight can be gained by solving Equation (S12) for the N_e consistent with the estimates of $\widetilde{p}_-$ obtained by computer simulation. Charlesworth (15) examined the Gaussian model mostly in the context of stabilizing selection, apparently with $L \leq 1000$ and quite strong selection, but a closed-form expression that he obtained for $\widetilde{p}_-$ (his Equation A3.a) does not closely track the results from simulations in the current study and yields $\widetilde{p}_- = 0$ in the absence of mutation bias. As can be seen in Figure S5, as a first-order approximation, the depression of N_e relative to N scales negatively as a power-law function of the ratio N/ω^2, i.e., with form

$$N_e/N = a(N/\omega^2)^b, \tag{S13}$$

with $N_e/N \simeq 1$ below a critical threshold value. In all cases, the fitted regressions account for $> 99\%$ of the variance in observed values, with the slopes of the logarithmic regressions always falling between -0.25 and -0.56.

The coefficients for this expression depend on the number of loci, the level of mutation bias, and the strength of selection in a somewhat complex way. By inspection, for the range of parameter space explored in the analyses ($\beta = 0.01$ to 1.0, $L = 10^3$ to 10^5, and $\omega = 7000$ to $41,000$), the normalizing factor is found to be

$$a \simeq \left(\frac{\omega}{667\beta L}\right)^{0.75} \cdot L^{-0.00005\omega}, \tag{S14a}$$

whereas the exponent is approximated by

$$b \simeq -0.08(\beta\omega)^{0.14} \cdot \omega^{0.01\log_{10}(L)}. \tag{S14b}$$

As with the exponential fitness function, with high intensities of selection relative to drift (large N/ω^2), N_e can be depressed by a factor as high as 1000, and the overall effect increases with increasing β and L. There are weak additional effects associated with the interaction of the strength of selection and the number of loci. It is desirable in future work to derive expressions such as these analytically.

Literature Cited

1. M. Kimura, T. Maruyama, J. F. Crow, The mutation load in small populations. *Genetics* **48,** 1303-1312 (1963).

2. S. Wright, *Evolution and the Genetics of Populations. Vol. 2. The Theory of Gene Frequencies.* (Univ. Chicago Press, 1969).

3. M. Abramowitz, I. A. Stegun (eds.), *Handbook of Mathematical Functions.* (Dover Publ., Inc., 1964).

4. B. Charlesworth, K. Jain, Purifying selection, drift, and reversible mutation with arbitrarily high mutation rates. *Genetics* **198,** 1587-1602 (2014).

5. G. Malécot, Les processes stochastiques et la méthode des fonctions génératrices ou caracteréstiques. *Publ. Inst. Stat. Univ. Paris 1: Fasc.* **3,** 1-16 (1952).

6. M. Kimura, Some problems of stochastic processes in genetics. *Ann. Math. Stat.* **28,** 882-901 (1957).

7. J. Haigh, The accumulation of deleterious genes in a population – Muller's Ratchet. *Theor. Popul. Biol.* **14,** 251-267 (1978).

8. P. Pfaffelhuber, P. R. Staab, A. Wakolbinger, Mullers ratchet with compensatory mutations. *Ann. Appl. Prob.* **22,** 2108-2132 (2012).

9. M. Lynch, R. Bürger, D. Butcher, W. Gabriel, Mutational meltdowns in asexual populations. *J. Heredity* **84,** 339-344 (1993).

10. K. Jain, S. John, Deterministic evolution of an asexual population under the action of beneficial and deleterious mutations on additive fitness landscapes. *Theor. Popul. Biol.* **112,** 117-125 (2016).

11. S. Goyal, *et al.,* Dynamic mutation-selection balance as an evolutionary attractor. *Genetics* **191,** 1309-1319 (2012).

12. G. Woodcock, P. G. Higgs, Population evolution on a multiplicative single-peak fitness landscape. *J. Theor. Biol.* **179,** 61-73 (1996).

13. S. John, K. Jain, Effect of drift, selection and recombination on the equilibrium frequency

of deleterious mutations. *J. Theor. Biol.* **365,** 238-246 (2015).

14. M. Lynch, Phylogenetic diversification of cell biological features. *Elife* **7,** e34820 (2018).

15. B. Charlesworth, Stabilizing selection, purifying selection, and mutational bias in finite populations. *Genetics* **194,** 955-971 (2013).

Figure S1. **a)** Observed within-population variances vs. predicted variances using Equation (S8b) after substituting the observed means from simulations. **b)** Observed phenotypic means vs. values predicted with Equation (S10) after substituting the observed within-population variances.

Figure S2. Comparison of long-term mean phenotypes (relative to the maximum value, L) observed with those predicted by the scaling relationships in Equations (1) and (11). Note that under the additive model used herein, the mean frequency of + alleles is equivalent to the fractional distance of the mean phenotype between 0 and L.

Figure S3. Ratio of effective and actual population sizes, as predicted by Equation (11) (solid lines) and determined by the means of the frequencies of + alleles from computer simulations applied to Equation (10), given for a range of segment lengths (numbers of linked sites, L) and mutation biases ($\beta = u_{01}/u_{10}$, with $s = 10^{-5}$ throughout.

Figure S4. Equilibrium mean frequency of the + alleles (equivalent to the mean phenotype $\widetilde{\mu}_m$, scaled to the maximum possible value, L) as a function of the absolute population size, with the number of loci $L = 10^5$ in all cases. Results, obtained by computer simulation, are given for three different levels of mutation bias and three strengths of selection for the half-Gaussian model, and compared to those for a shallower exponential fitness function. Mutation rates are defined by the empirical scaling relationship noted in the text.

Figure S5. Scaling of the effective population size relative to the expectation with no selective interference (N_e/N) with respect to the ratio of the strength of selection relative to drift (N/ω^2) for the case of a half-Gaussian directional selection function. Results were obtained as long-term averages from Wright-Fisher computer simulations, by substituting long-term mean allele frequencies into Equation (24) and solving for N_e; the straight lines are linear least-squares regressions for the downhill slopes of the data.

Figure S1

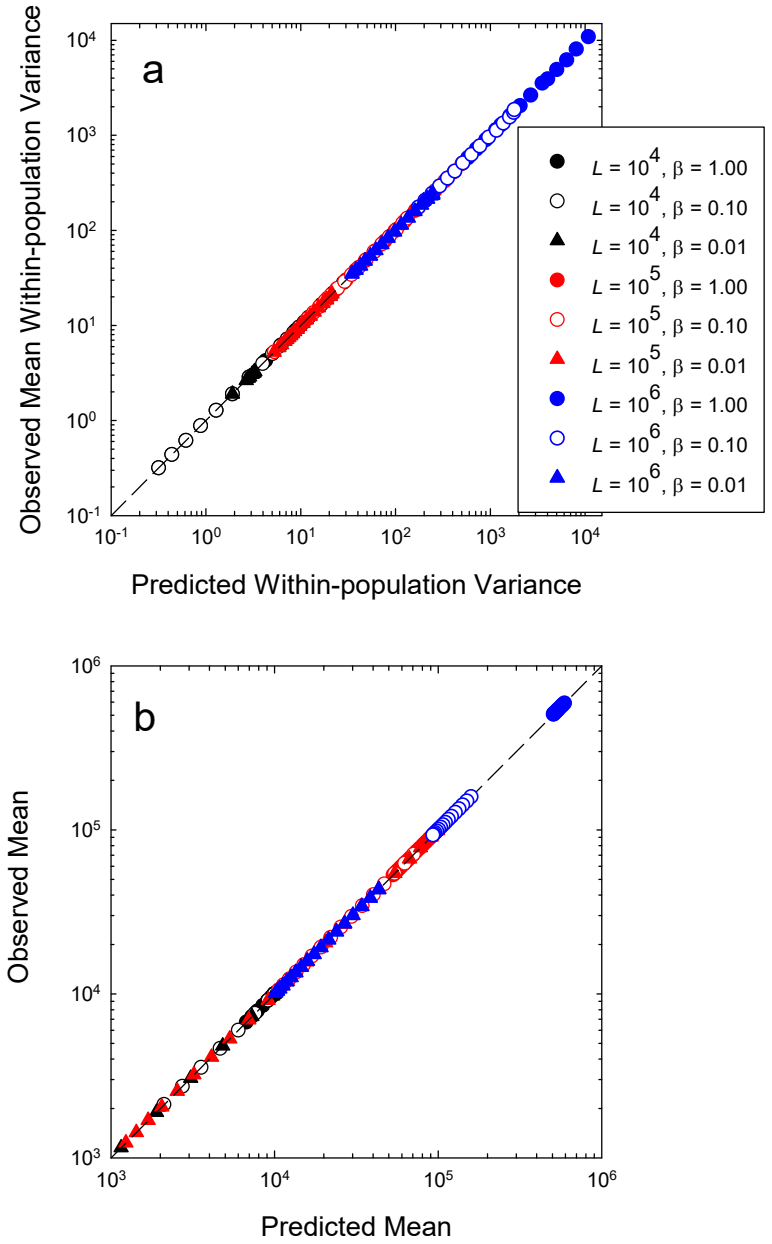
a
Observed Mean Within-population Variance
Predicted Within-population Variance
10^{-1}
10^{0}
10^{1}
10^{2}
10^{3}
10^{4}
$L = 10^4$, β = 1.00
$L = 10^4$, β = 0.10
$L = 10^4$, β = 0.01
$L = 10^5$, β = 1.00
$L = 10^5$, β = 0.10
$L = 10^5$, β = 0.01
$L = 10^6$, β = 1.00
$L = 10^6$, β = 0.10
$L = 10^6$, β = 0.01
b
Observed Mean
Predicted Mean
10^{3}
10^{4}
10^{5}
10^{6}

Figure S2

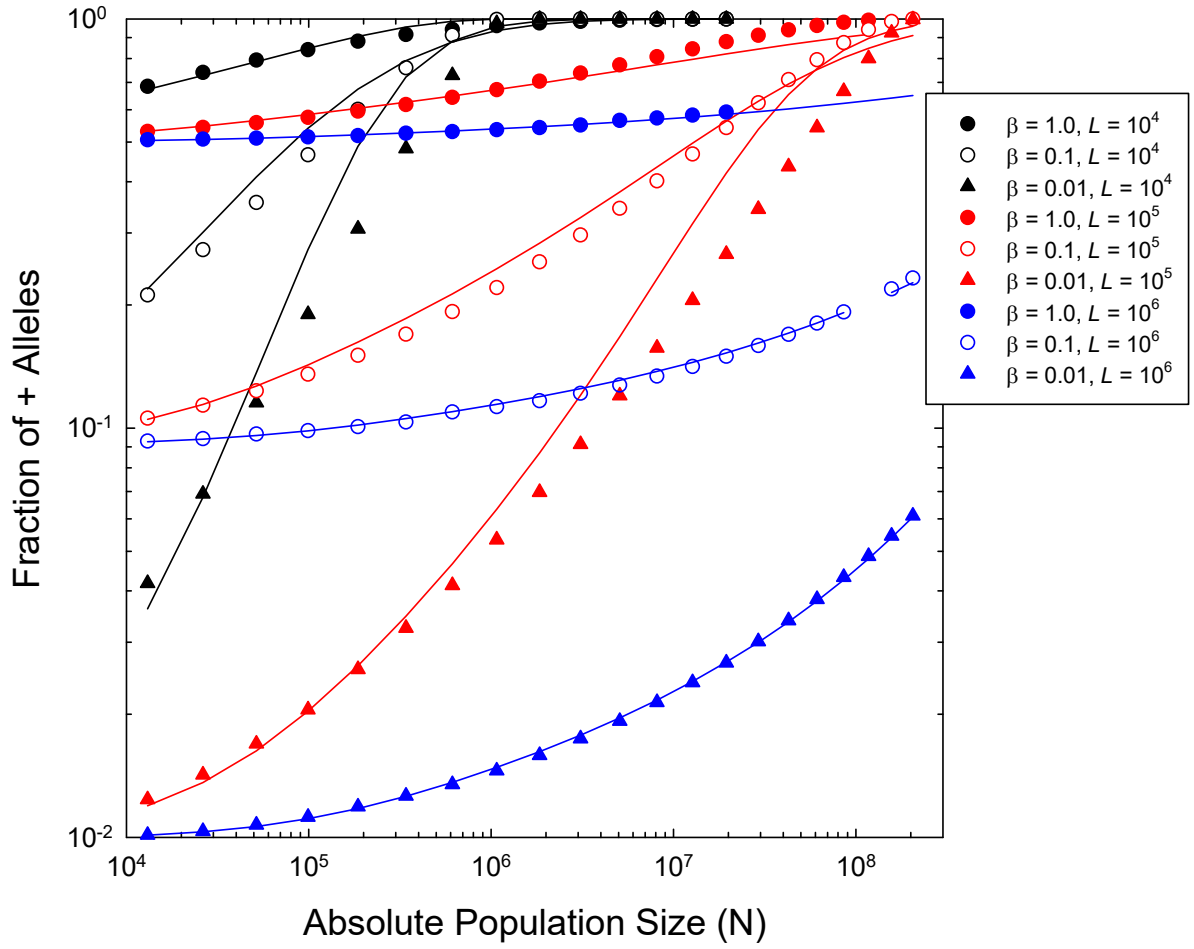
Fraction of + Alleles
Absolute Population Size (N)
10^0
10^{-1}
10^{-2}
10^4
10^5
10^6
10^7
10^8
β = 1.0, L = 10^4
β = 0.1, L = 10^4
β = 0.01, L = 10^4
β = 1.0, L = 10^5
β = 0.1, L = 10^5
β = 0.01, L = 10^5
β = 1.0, L = 10^6
β = 0.1, L = 10^6
β = 0.01, L = 10^6

Figure S3

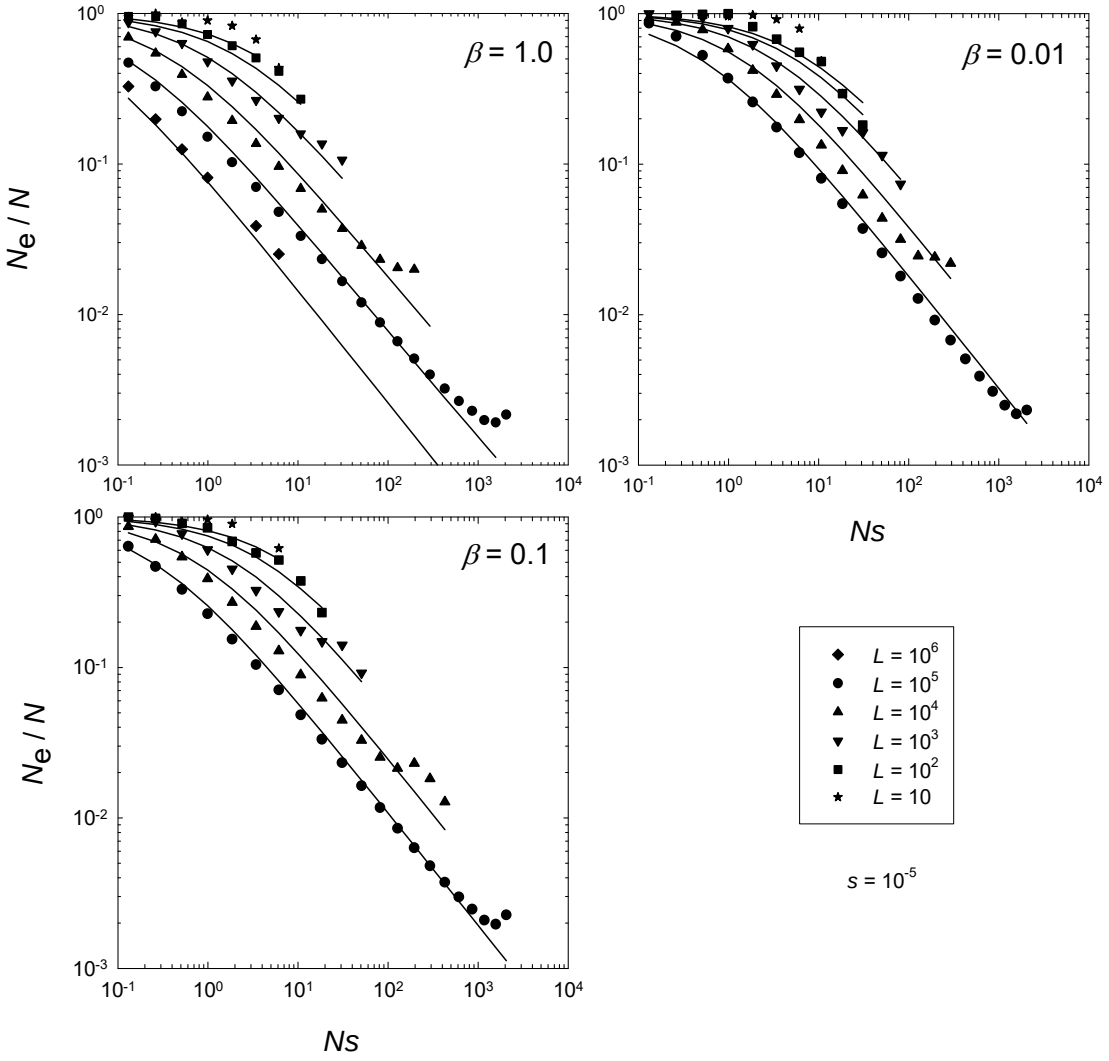

Figure S4

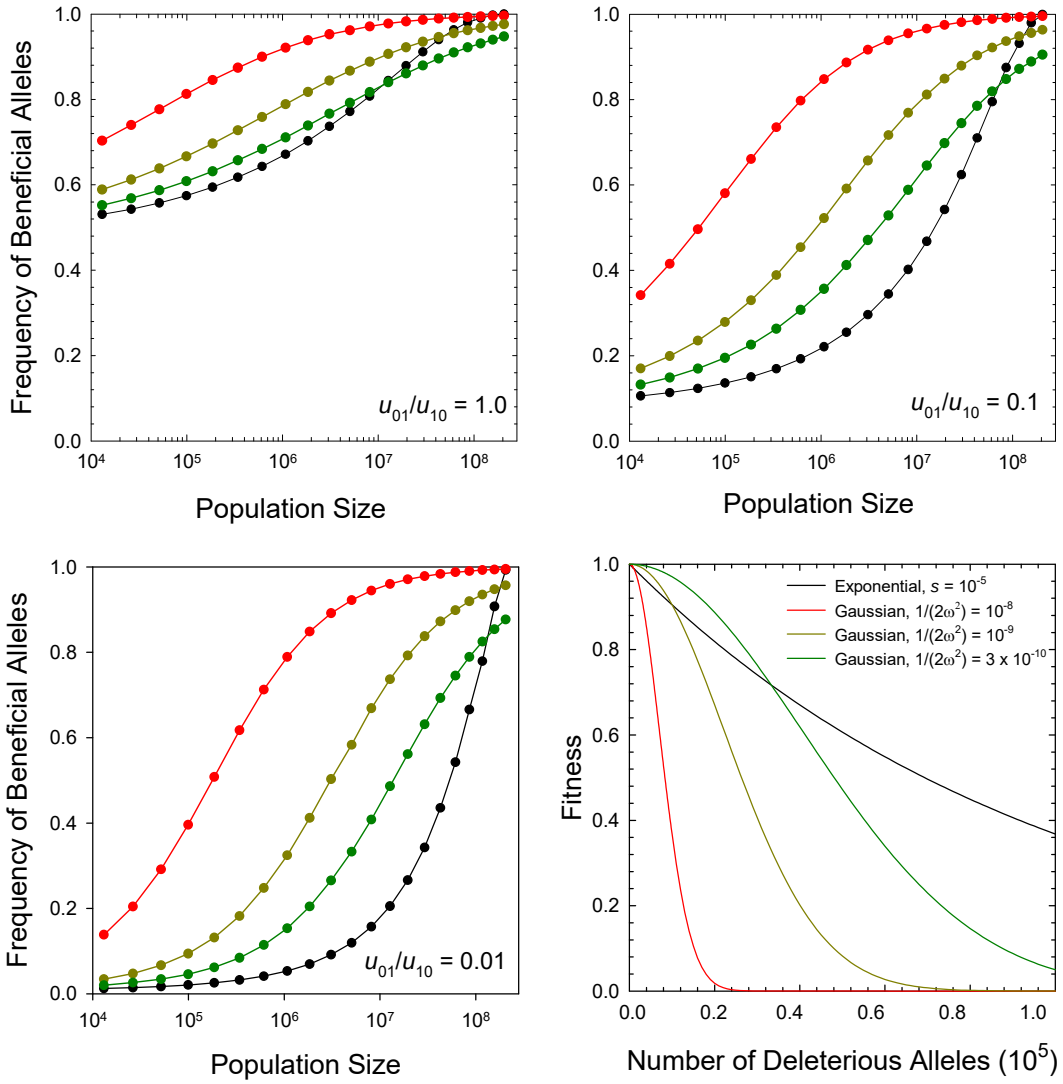
Frequency of Beneficial Alleles
Population Size
u_{01}/u_{10} = 1.0
u_{01}/u_{10} = 0.1
u_{01}/u_{10} = 0.01
Fitness
Number of Deleterious Alleles (10^5)
Exponential, $s = 10^{-5}$
Gaussian, $1/(2\omega^2) = 10^{-8}$
Gaussian, $1/(2\omega^2) = 10^{-9}$
Gaussian, $1/(2\omega^2) = 3 \times 10^{-10}$

Figure S5

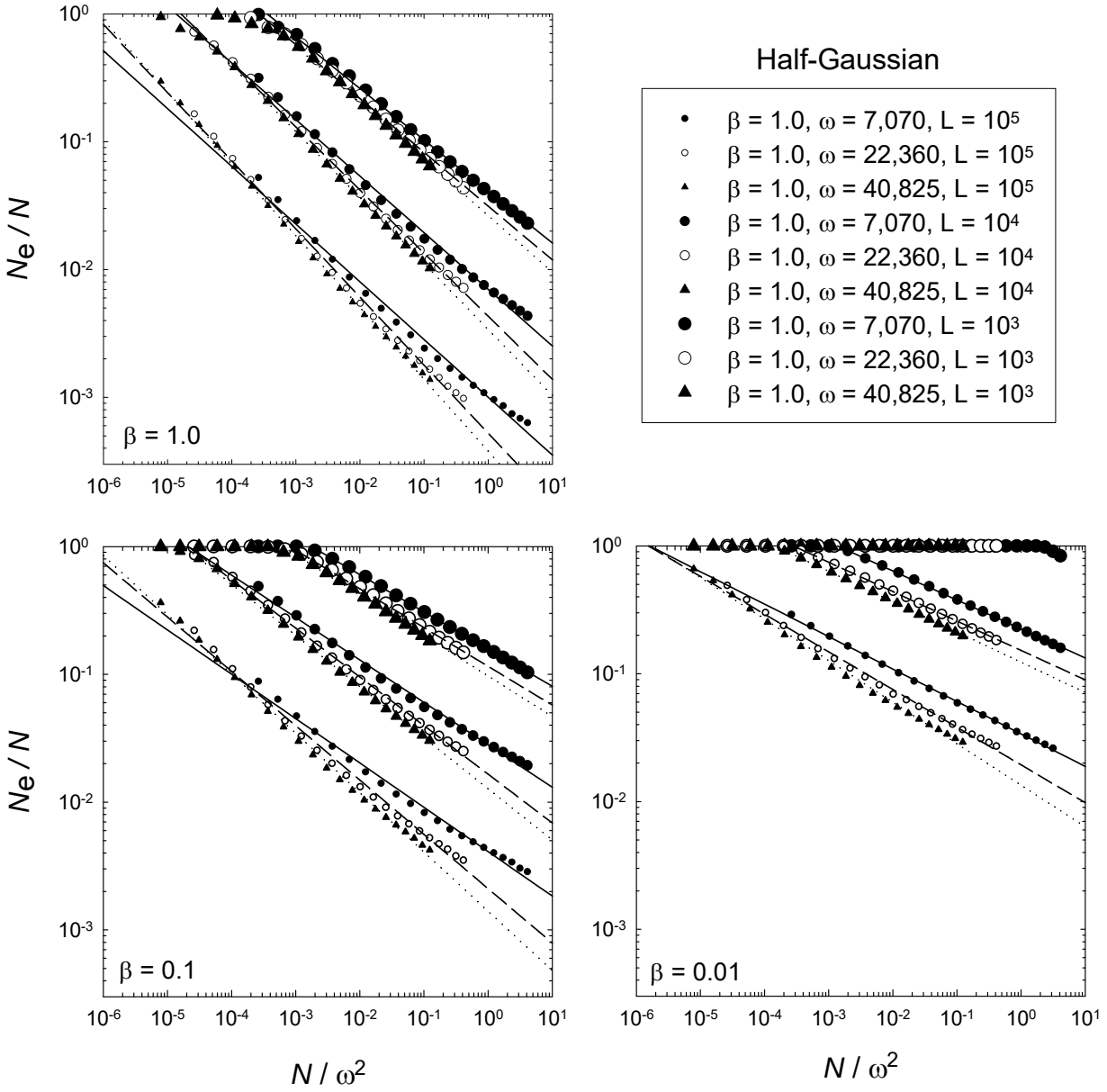
Half-Gaussian
β = 1.0, ω = 7,070, L = 10^5
β = 1.0, ω = 22,360, L = 10^5
β = 1.0, ω = 40,825, L = 10^5
β = 1.0, ω = 7,070, L = 10^4
β = 1.0, ω = 22,360, L = 10^4
β = 1.0, ω = 40,825, L = 10^4
β = 1.0, ω = 7,070, L = 10^3
β = 1.0, ω = 22,360, L = 10^3
β = 1.0, ω = 40,825, L = 10^3
Ne / N
β = 1.0
β = 0.1
β = 0.01
N / ω^2